Virologica Sinica 40 (2025) 340–348

Contents lists available at ScienceDirect

Virologica Sinica

journal homepage: www.keaipublishing.com/en/journals/virologica-sinica
www.virosin.org

Research Article

Viral pseudo-enzyme facilitates KSHV lytic replication via suppressing PFAS-mediated RTA deamidation

Yang Xu [a,1], Qiushi Zhang [a,1], Guoli Hou [a,b], Liang Hu [a], Tiaoyi Xiao [a], Xinyu Liang [a], Deliang Li [a,*], Junhua Li [a,*]

[a] College of Fisheries, Hunan Agricultural University, Changsha, 410128, China
[b] Section of Infection and Immunity, Herman Ostrow School of Dentistry, University of Southern California, Los Angeles, CA 90089, USA

ARTICLE INFO

Keywords:
Kaposi's sarcoma-associated herpesvirus (KSHV)
viral glutamine amidotransferase (vGAT)
transcription activator (RTA)
Deamidation

ABSTRACT

Deamidation, a type of post-translational modification commonly considered a hallmark of protein "aging" and function decay, is increasingly recognized for its pivotal role in regulating biological processes and viral infection. Our previous study has demonstrated that the deamidation of replication and transcription activator (RTA), a master regulator of ubiquitous and oncogenic Kaposi's sarcoma-associated herpesvirus (KSHV), mediated by phosphoribosylformylglycinamidine synthetase (PFAS), hinders its nuclear import and transcriptional activity. Here we report that the viral glutamine amidotransferase (vGAT) pseudo-enzyme is exploited to facilitate KSHV lytic infection by inhibiting RTA deamidation. To be more specific, vGAT interacts with both RTA and cellular PFAS, and inhibits PFAS-mediated RTA deamidation, thus facilitating RTA nuclear localization and suppressing nuclear factor-kappa B (NF-κB) signaling activation, as well as augmenting RTA-mediated transcriptional activation of viral open reading frames (ORFs). In addition, vGAT appears to regulate the deamidation process of several viral ORFs of KSHV. Collectively, these findings unveil that a viral pseudo-enzyme is exploited to enhance viral infection via deamidation regulation.

INTRODUCTION

Kaposi's sarcoma-associated herpesvirus (KSHV) is an oncogenic gamma-herpesvirus intimately involved in human diseases, with a life cycle that consists of a latent infection phase and a lytic replication phase (Chang et al., 1994; Ye et al., 2011; Broussard and Damania, 2020). During KSHV lytic replication, viral open reading frames (ORFs), such as polyadenylated nuclear (PAN), ORF45, ORF50, ORFK8, ORFK9, ORF57, ORF59, ORF25, and ORF65, are expressed in a cascade manner (Broussard and Damania, 2020; Arias et al., 2014; Yang et al., 2022). As an immediate-early gene product, replication and transcription activator (RTA), encoded by ORF50, initiates the expression of multiple genes associated with replication and pathogenesis of gamma-herpesvirus like KSHV, as well as mediating the switch of the viral cycle from latency to lytic replication (Sun et al., 1998). Besides transcriptional activation, RTA also regulates cytokine activity and modulates immunity. For example, RTA facilitates ubiquitination and degradation of interferon regulatory factor (IRF-7), thereby perturbing the production of type I interferons (IFNs) (Yu et al., 2005). RTA also interacts with myeloid differentiation factor 88 (MyD88) and degrades MyD88 via the ubiquitin-proteasome pathway, eliciting blockade of TLR signaling and associated antiviral dysfunction (Zhao et al., 2015).

Protein function is generally regulated by a variety of post-translational modifications, such as acetylation, methylation, ubiquitination, and deamidation. Extensive studies have established potential relationships between gain- or loss-of-function and RTA modifications. For example, manipulated N^6-adenosine methylation (m^6A) mediates the splicing of the pre-mRNA encoding the RTA, thereby modulating KSHV lytic replication (Ye et al., 2017). Besides, RTA promoter histone acetylation rather than demethylation regulates murine gamma-herpesvirus 68 (MHV68) reactivation (Yang et al., 2009). Deubiquitination and stabilization of RTA by recruiting host deubiquitinases (OTUD4 and USP7)

* Corresponding authors.
E-mail addresses: lidl@hunau.edu.cn (D. Li), lijunhua@hunau.edu.cn (J. Li).
[1] Yang Xu and Qiushi Zhang contributed equally to this work.

https://doi.org/10.1016/j.virs.2025.04.005
Received 16 November 2024; Accepted 9 April 2025
Available online 12 April 2025

facilitate KSHV lytic reactivation (Wang et al., 2024). Conversely, ubiquitination and degradation of RTA by interacting with RNF213 inhibits the *de novo* infection and lytic reactivation of KSHV (Tian et al., 2023). Even though deamidation of proteins is no longer an emerging topic, it remains widely recognized as protein "aging" or functional decay, and our insight into the exact functions of deamidation remains confined (He et al., 2015). To the best of our knowledge, no attention has been focused on the modulation of RTA function by deamidation beyond our previous study (Li et al., 2019).

Our previous study has illustrated that phosphoribosylformylglycinamidine synthetase (PFAS) deamidates RTA and diminishes RTA nuclear localization and transcriptional activation, thereby inhibiting KSHV lytic replication (Li et al., 2019). As a member of the glutamine amidotransferase (GAT) family, PFAS is generally recognized as a deamidase widely involved in the biosynthesis of nucleotides, amino acids, and lipids (Lu et al., 2019). Interestingly, the gamma-herpesvirus genome also encodes viral GAT (vGAT), sharing homology with cellular PFAS but deficient in intrinsic amidotransferase activity. As a pseudo-enzyme, vGAT exerts crucial roles in mediating innate immune evasion of gamma-herpesviruses. It has been demonstrated that vGAT is exploited to recruit cellular PFAS to deamidate retinoic acid-induced gene I (RIG-I) and negate cytokine production during MHV68 infection (He et al., 2015).

Herein, we demonstrate that KSHV-encoded vGAT augments viral replication by suppressing PFAS-mediated RTA deamidation. This finding underscores the significance of deamidation regulation on viral pathogenic mechanisms and positions deamidation modulation as a promising target for antiviral prophylaxis.

RESULTS

vGAT interacts with both RTA and cellular PFAS

We previously reported that PFAS interacts with and deamidates RTA (Li et al., 2019). Given that vGAT is a glutamine amidotransferase homologous to cellular PFAS, we thus speculated that vGAT might interact with RTA and cellular PFAS, and regulate the deamidation of RTA. Gel filtration also hinted at potential relationships among PFAS, RTA, and vGAT (Fig. 1A). To validate this hypothesis, we first checked the interaction of vGAT with its cellular counterpart, PFAS. Interestingly, as a pseudo-enzyme, vGAT does not possess intrinsic enzyme activity but interacted with PFAS (Fig. 1B), indicating a potential role in modulating PFAS-mediated RTA deamidation. The interaction between vGAT and RTA was then explored. In transfected 293T cells, vGAT co-precipitated with exogenous RTA (Fig. 1C), and in reactivated iSLK/iBAC16 cells, vGAT co-precipitated with endogenous RTA (Fig. 1D). Moreover, an interaction among exogenously expressed vGAT, RTA, and PFAS was detected (Fig. 1E). Together, these results suggest that an interaction among vGAT, RTA and cellular PFAS is identified.

vGAT inhibits RTA deamidation

Since we have confirmed the interaction of vGAT, PFAS, and RTA, to further verify the above hypothesis, we investigated the effect of vGAT on RTA deamidation. Reporter assays indicated that vGAT facilitated the RTA-mediated transcriptional activation of pPAN, pORF57, and pvIL-6 promoters in a dose-dependent manner (Fig. 2A). Next, we overexpressed vGAT and monitored RTA charge status. Overexpression of vGAT shifted RTA-WT toward the negative pole (Fig. 2B), suggesting a charge shift induced by inhibition of RTA deamidation. To determine the site(s) of deamidation, RTA was purified from transfected 293T cells without or with vGAT and analyzed by tandem mass spectrometry (MS) (Fig. 2C). Two peptides were determined that contained deamidated residues of N37 and N225, which were specifically repressed by vGAT (Fig. 2D, Supplementary Fig. S1). When a two-site deamidated RTA mutant of residues N37 and N225 (RTA-DD) was introduced, vGAT failed to further shift RTA-DD (Fig. 2B). Together, these results suggests that vGAT inhibits the deamidation of RTA, thereby facilitating RTA-mediated transcriptional activation.

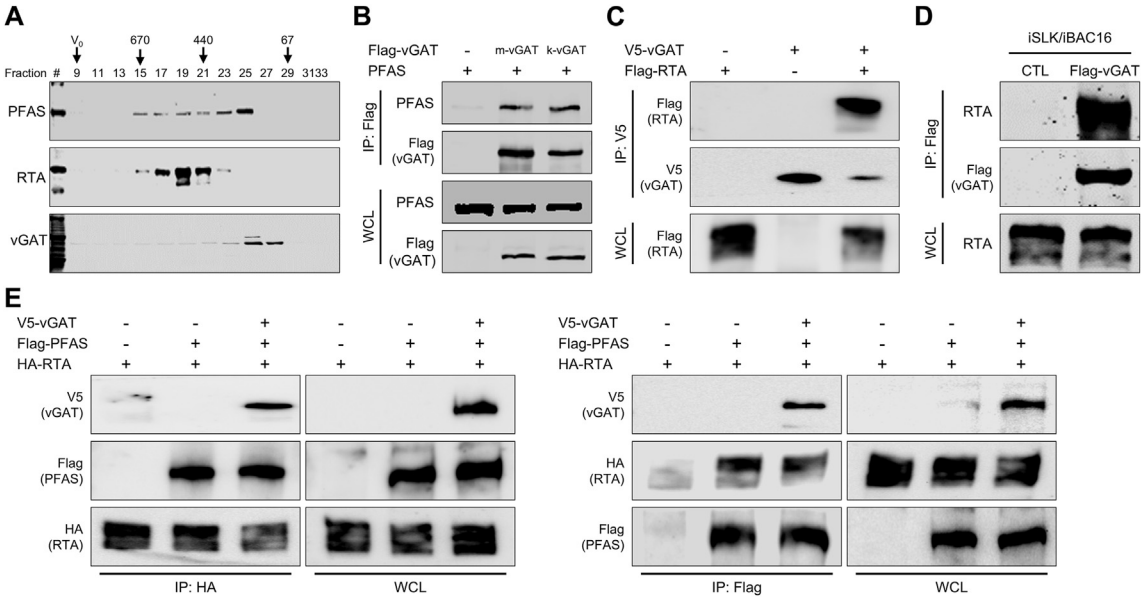

Fig. 1. vGAT interacts with both RTA and cellular PFAS. **A** 293T cells were infected with KSHV (multiplicity of infection, MOI = 5) for 24 h. Purified PFAS, RTA, and vGAT were analyzed by gel filtration. **B** 293T cells were transfected with plasmids expressing MHV68 (m-vGAT) or KSHV (k-vGAT) GAT and plasmids expressing PFAS. Whole-cell lysates (WCLs) were prepared and immunoprecipitation was performed. Precipitated proteins and WCLs were analyzed by immunoblotting with indicated antibodies. **C** 293T cells were transfected with indicated plasmids. WCLs were prepared and immunoprecipitation was performed. Precipitated proteins and WCLs were analyzed by immunoblotting with indicated antibodies. **D** iSLK/iBAC16 cells were induced with doxycycline (1 μg/mL) for 48 h. WCLs were prepared and immunoprecipitation was performed. Precipitated proteins and WCLs were analyzed by immunoblotting with indicated antibodies. **E** 293T cells were transfected with indicated plasmids. WCLs were prepared and immunoprecipitation was performed. Precipitated proteins and WCLs were analyzed by immunoblotting with indicated antibodies.

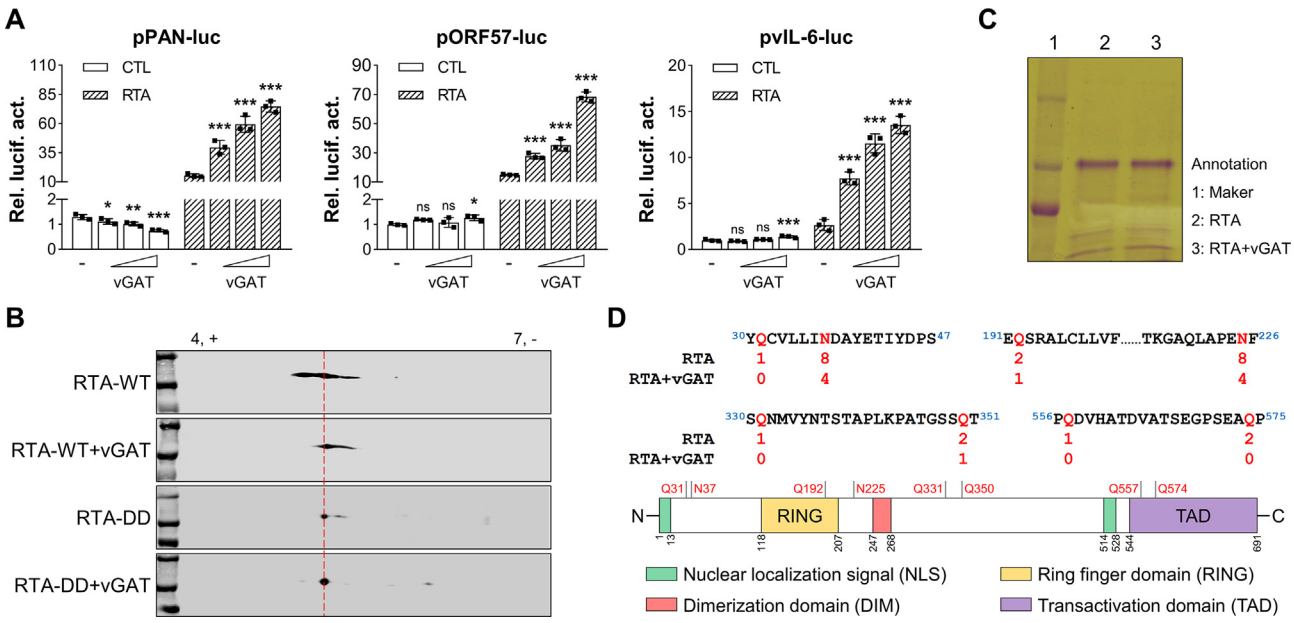

Fig. 2. vGAT inhibits the deamidation of RTA. **A** 293T cells were transfected with indicated reporter cocktails and different dose of plasmids expressing vGAT (1 ng, 10 ng, and 50 ng) without or with RTA (1 ng). vGAT mediated RTA-dependent transcriptional activation of the indicated promoters was determined by luciferase reporter assay. Data presented as mean ± standard deviations. Statistical analyses were performed using one-way analysis of variance (ANOVA). Statistical significance was set at $^{*}P < 0.05$, $^{**}P < 0.01$, $^{***}P < 0.001$, while "ns" indicated "not significant". **B** 293T cells were transfected with plasmids expressing wild type RTA (RTA-WT) or RTA deamidation mutant (RTA-DD) without or with vGAT. WCLs were analyzed by two-dimensional gel electrophoresis and immunoblotting. **C** 293T cells were transfected with plasmids expressing RTA without or with vGAT. RTA was purified via single step affinity chromatography using anti-FLAG M2 agarose and eluted with FLAG peptide (0.2 mg/mL). Proteins remained on beads were analyzed by SDS-PAGE and Coomassie staining. The RTA band was excised and analyzed by tandem mass spectrometry (MS). **D** RTA was purified from transfected 293T cells with plasmids expressing RTA without or with vGAT and analyzed by tandem MS for deamidation. Two deamidated residues (N37 and N225) specifically inhibited by vGAT were identified (top). The structural domains of RTA are diagrammed (bottom).

Deamidation impairs RTA-mediated transcriptional activation of viral ORFs

To further investigate the impact of RTA deamidation during KSHV infection, RTA-DD was introduced in reporter assays. The results showed that RTA-DD greatly impaired the transcription of pORF57 and pvIL-6, and completely failed to activate the pPAN compared to RTA-WT (Fig. 3A). In addition, iSLK.RTA.219 system was introduced (Fig. 3B), which induces KSHV reactivation by doxycycline and indicates viral latent infection and lytic replication with green and red fluorescence signals, respectively. Interestingly, despite the higher expression of RTA-DD than RTA-WT with the corresponding dose of doxycycline (Fig. 3D), the lytic replication of KSHV.219 was ~1.5- to 3-fold significantly lower in iSLK.DD.219 cells than that in iSLK.WT.219 cells, as indicated by normalized fluorescence intensity (Fig. 3C). The expression of PAN, ORF21, and ORF59 in iSLK.DD.219 cells was ~5- to 35-fold significantly lower than that in iSLK.WT.219 cells (Fig. 3E). Moreover, viral genome level was ~1.5- to 3-fold significantly lower in iSLK.DD.219 cells than that in iSLK.WT.219 cells (Fig. 3F). Notably, the above phenotypes of RTA-DD may not be adequately demonstrated since KSHV genome-expressed RTA-WT could compensate for RTA-DD-induced loss of function. Nevertheless, these results illustrate that deamidation impairs RTA-mediated transcriptional activation of viral ORFs during KSHV lytic replication.

Inhibition of deamidation promotes RTA-mediated transcriptional activation of viral ORFs

Our previous study has confirmed that N to Q mutations reinforce RTA resistance to PFAS-mediated deamidation (Li et al., 2019). A deamidation-resistant RTA mutant (RTA-N37Q) was then utilized to probe the effects of RTA deamidation during KSHV infection from a reverse perspective. As expected, RTA-N37Q significantly induced transcriptional activation at all promoters compared to RTA-WT (Fig. 4A). In addition, the HOK.iBAC.RTA system was introduced (Fig. 4B). Interestingly, despite the lower expression of RTA-N37Q than RTA-WT (Fig. 4D), infectious virions in the supernatant of SLK.iBAC.N37Q cells were higher than that of HOK.iBAC.WT cells (Fig. 4C). The expression of PAN, ORF25, and ORF59 in HOK.iBAC.N37Q cells was one to two orders of magnitude higher than that in HOK.iBAC.WT cells (Fig. 4E). Furthermore, the viral genome level of HOK.iBAC.N37Q cells was ~5-fold significantly higher than that of HOK.iBAC.WT cells (Fig. 4F). Together, these results demonstrate in reverse that deamidation impairs RTA-mediated transcriptional activation of viral ORFs during KSHV lytic replication.

Deamidation blocks RTA nuclear translocation

We previously reported that RIG-I bound RTA and blocked its nuclear translocation, thus repressing viral replication (Xu et al., 2023). It was then hypothesized that deamidation might block the nuclear translocation of RTA, thus impairing RTA-mediated transcriptional activation. According to subcellular fractionation, ~90% of RTA-WT was localized in the nucleus, whereas only ~10% of RTA-DD was localized in the nucleus (Fig. 5A). In addition, RTA-WT was predominantly localized in the nucleus at the early stage of induction, whereas it was extensively retained in the cytoplasm at 72 h after induction (Fig. 5B), indicating that endogenous deamidation during KSHV reactivation might block the nuclear translocation of RTA. However, the localization of RTA-DD in the cytoplasm and nucleus was comparable at 24 h and 72 h after doxycycline induction and no significant nuclear translocation trend was observed (Fig. 5C), indicating that RTA-DD might not undergo endogenous deamidation. Consistently, immunofluorescence microscopy presented intuitive results (Fig. 5B–C). Together, these results demonstrated that deamidation blocked the nuclear translocation of RTA.

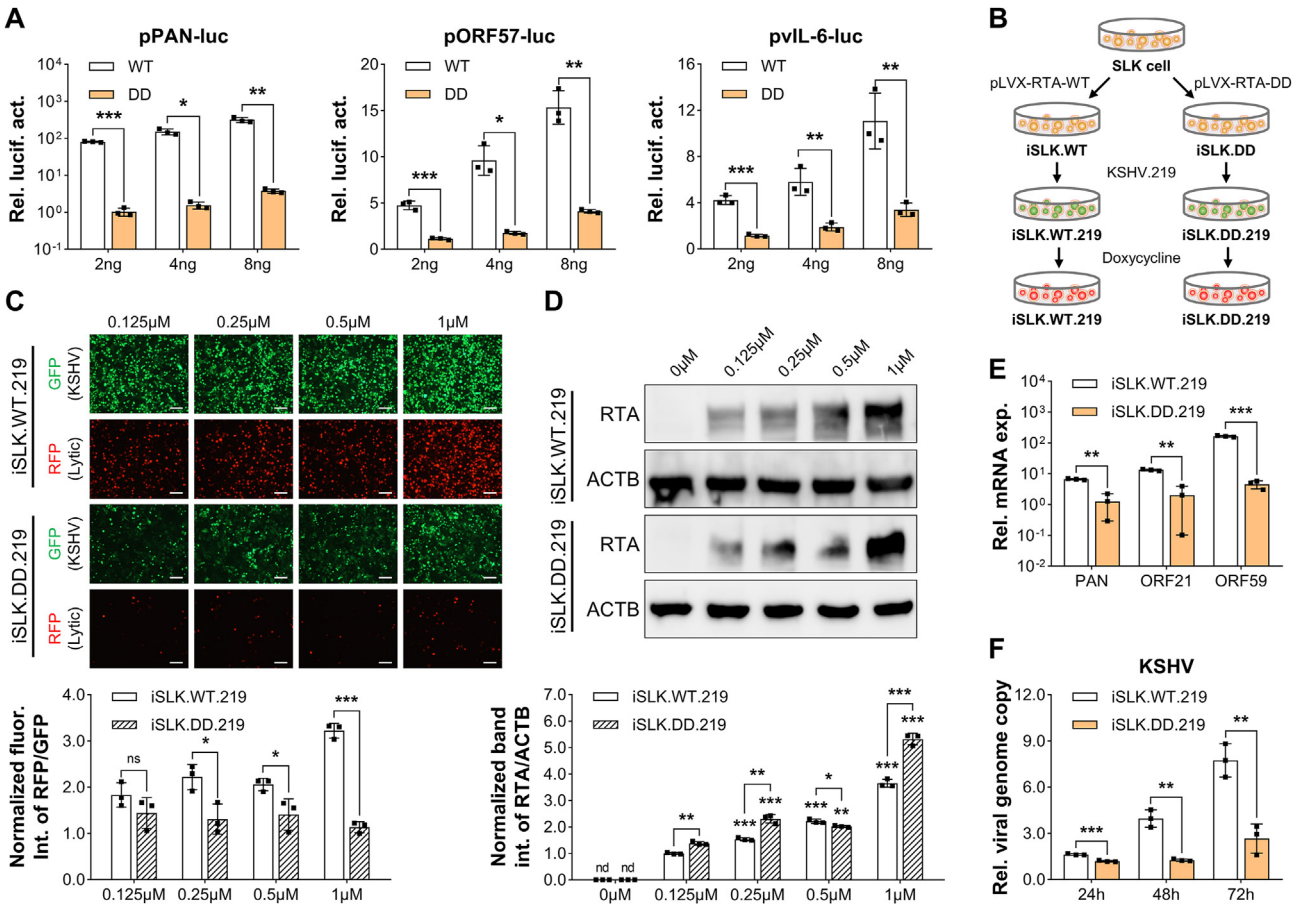

Fig. 3. Deamidation impairs RTA-mediated transcriptional activation and expression of viral ORFs. **A** 293T cells were transfected with the indicated reporter cocktails and the indicated dose of plasmids expressing RTA-WT or RTA-DD. RTA-dependent transcriptional activation of the indicated promoters was determined by luciferase reporter assay. **B** Graphic depicting the establishment of iSLK.WT.219 and iSLK.DD.219 stable cell lines. **C** iSLK.WT.219 and iSLK.DD.219 cells were induced with different dose of doxycycline and analyzed by fluorescence microscope (top). The fluorescence intensity of RFP/GFP was normalized to quantify KSHV lytic replication (bottom). **D** iSLK.WT.219 and iSLK.DD.219 cells were induced with different dose of doxycycline and harvested to detect RTA protein expression by immunoblotting (top). The band intensity of RTA/ACTB was normalized to quantify RTA protein expression (bottom). **E** iSLK.WT.219 and iSLK.DD.219 cells were induced with doxycycline (1 μg/mL) for 24 h and harvested to quantify the relative expression of the indicated gene by qPCR analysis. **F** iSLK.WT.219 and iSLK.DD.219 cells were induced with doxycycline (1 μg/mL) for the indicated times and harvested to quantify the relative viral genome copy by qPCR analysis using primers specific for ORF75. Data presented as mean ± standard deviations. Statistical analyses were performed using Student's *t*-test or one-way analysis of variance (ANOVA). Statistical significance was set at $^{*}P < 0.05$, $^{**}P < 0.01$, $^{***}P < 0.001$, while "ns" indicated "not significant".

Deamidation rescues RTA-induced repression of NF-κB signaling activation

NF-κB signaling is a canonical pro-inflammatory pathway, whereas IFN signaling is a classical antiviral pathway. We then investigated the impact of RTA deamidation on NF-κB and IFN signaling. Immunoblotting analysis showed that deamidation rescued RTA-induced reduction in RelA, IRF3, and IRF7 protein levels as well as the phosphorylation of P65 (Fig. 5D–F). Reporter assays indicated that deamidation rescued the RTA-induced repression of transcriptional activation of the NF-κB promoter but not the IFN-β promoter (Fig. 5G and H). Together, these results demonstrate that deamidation rescues RTA-induced repression of NF-κB signaling activation.

vGAT inhibits the deamidation of viral ORFs of KSHV

Lastly, we overexpressed vGAT and monitored viral ORFs, including ORF45, ORF59, ORFK9, and ORFK8 charge statuses. Overexpression of vGAT shifted ORF45, ORF59, and ORFK9 toward the negative pole (Fig. 6A–C), suggesting a charge shift induced by inhibition of viral ORFs deamidation. However, vGAT appeared to fail to alter the charge of ORFK8 (Fig. 6D). Together, these results demonstrated that besides RTA, vGAT might also inhibit the deamidation of several viral ORFs of KSHV.

DISCUSSION

PFAS is a highly conserved enzyme belonging to the GAT family, and catalyzes the purine synthesis pathway (He et al., 2015). Several studies have demonstrated that PFAS mediates the deamidation of RIG-I, RTA, and phosphoglycerate dehydrogenase (PHGDH) (He et al., 2015; Li et al., 2019; Lu et al., 2019). Although traditionally recognized as a signature of protein "aging" and functional decay, emerging evidence has been proposed to illustrate that deamidation regulates host antiviral immunity during pathogenic infection (Zhao et al., 2016a; Xie et al., 2024). For example, deamination of RIG-I and cGAS mediated by the herpes simplex virus 1 (HSV-1) UL37 tegument protein arrests downstream innate immune activation (Zhao et al., 2016b; Zhang et al., 2018). CTP synthase 1 (CTPS1) deamidates IRF3 to mute IFN induction (Rao et al., 2021). The initiation of glycolysis and the shutdown of inflammation mediated by deamination of RelA, a subunit of NF-κB, facilitates viral replication and persistent infection (Zhao et al., 2020; Qin et al., 2022; Wan et al., 2024). vGAT, homologous to cellular PFAS, is regarded as a viral pseudo-enzyme due to the absent catalytic activity (He et al., 2015). Several studies have

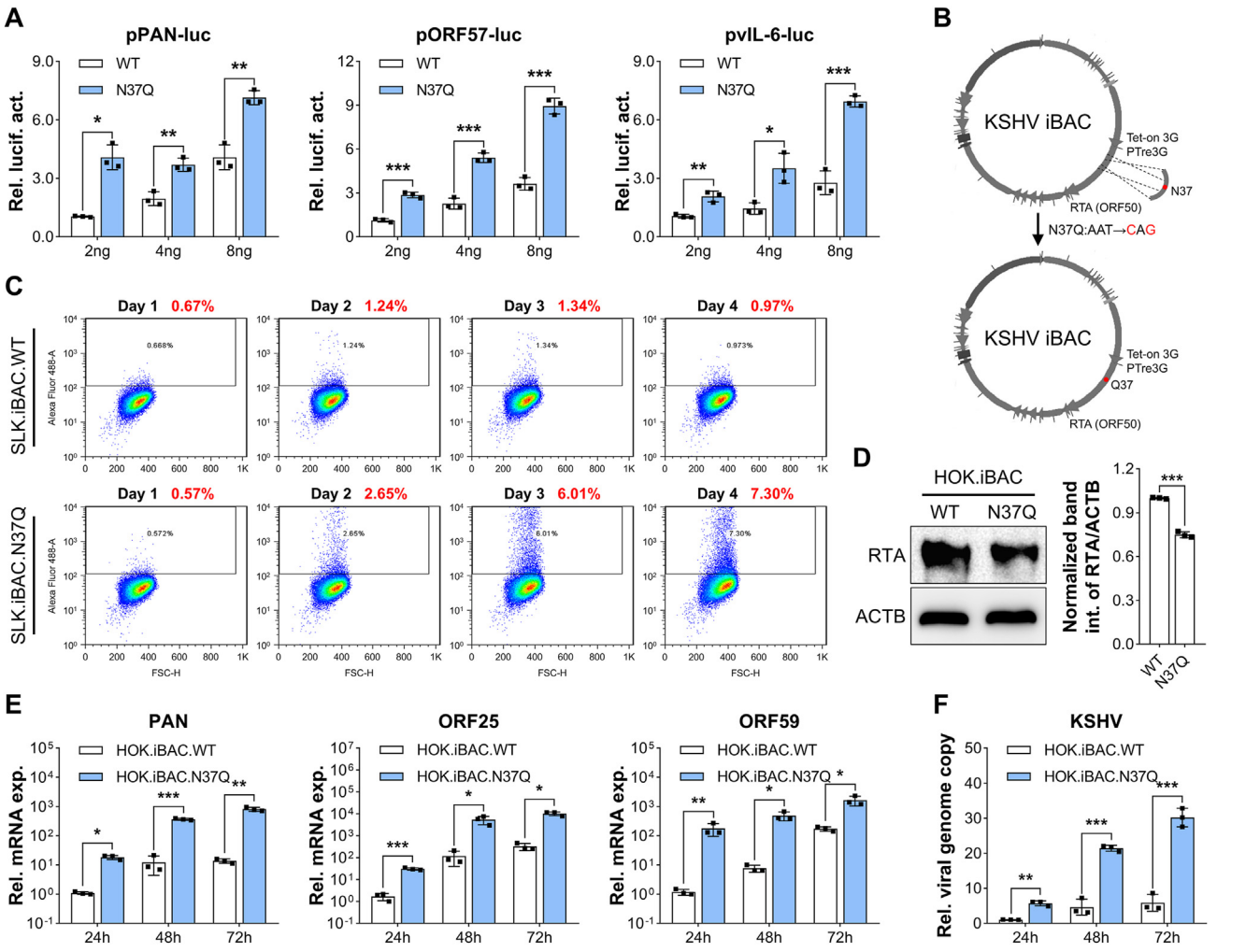

Fig. 4. Inhibition of deamidation promotes RTA-mediated transcriptional activation and expression of viral ORFs. **A** 293T cells were transfected with the indicated reporter cocktails and the indicated dose of plasmids expressing RTA-WT or deamidation-resistant RTA mutant (RTA-N37Q). RTA-dependent transcriptional activation of the indicated promoters was determined by luciferase reporter assay. **B** Graphic depicting the establishment of SLK or HOK cells carrying KSHV iBAC with RTA-WT or RTA-N37Q. **C** SLK.iBAC.WT and SLK.iBAC.N37Q cells were induced with doxycycline (1 μg/mL) for the indicated times. Infectious virions in the supernatant were quantified by flow cytometry. **D** HOK.iBAC.WT and HOK.iBAC.N37Q cells were induced with doxycycline (1 μg/mL) and harvested to detect RTA protein expression by immunoblotting (left). The band intensity of RTA/ACTB was normalized to quantify RTA protein expression (right). **E** HOK.iBAC.WT and HOK.iBAC.N37Q cells were induced with doxycycline (1 μg/mL) for the indicated times and harvested to quantify the relative expression of the indicated genes by qPCR analysis. **F** HOK.iBAC.WT and HOK.iBAC.N37Q cells were induced with doxycycline (1 μg/mL) for the indicated times and harvested to quantify the relative viral genome copy by qPCR analysis using primers specific for ORF75. Data presented as mean ± standard deviations. Statistical analyses were performed using Student's *t*-test. Statistical significance was set at $^{*}P < 0.05$, $^{**}P < 0.01$, $^{***}P < 0.001$, while "ns" indicated "not significant".

demonstrated that pseudo-enzymes are widely involved in viral infection and host immunity (Wang et al., 2020). For example, vaccinia virus B1 kinase and B12 pseudo-kinase constitute a paired kinase/pseudo-kinase system to regulate the phosphorylation of cellular barrier to auto-integration factor (BAF) and related viral DNA replication (Olson et al., 2019; Rico et al., 2019, 2021). The competition between cellular superoxide dismutase (SOD) and viral pseudo-dismutase impairs cellular dismutase activity, causing superoxide overload, which represses Fas-mediated apoptosis and encourages the proliferation of infected cells (Teoh et al., 2005). Our previous study has also revealed that MHV68 vGAT binds and recruits cellular PFAS to trigger the deamidation and subsequent activation of RIG-I (He et al., 2015). In the current study, the interaction among vGAT, RTA, and cellular PFAS was identified. Since PFAS interacts with and deamidates RTA (Li et al., 2019), the interaction of vGAT with RTA and PFAS might account for the attenuated PFAS-mediated deamidation of RTA.

RTA, the initiator of the lytic replication program of gamma herpesviruses, determines the fate of the infected cell. Accumulating studies have pointed to RTA as a critical regulatory node in the process of gamma herpesvirus infection. For example, RTA interacts with and degrades inhibitor of DNA binding protein 2 (ID2), structural maintenance of chromosome (SMC) complex 5/6, and tripartite motif 32 (TRIM32) via hijacking the ubiquitin-proteasome system, allowing for the reactivation of KSHV lytic replication and virion production (Combs et al., 2022; Han et al., 2022; Zhang et al., 2024). RTA binds and recruits the E3 ubiquitin-protein ligase RNF20/40 complex for the persistent expression of RTA, thus pushing forward the lytic cycle and the transactivation of viral genes (Spires et al., 2023). The function of proteins is generally subject to an array of post-translational modifications, which is also the case for RTA. Extensive studies have defined that post-translational modifications regulate the gain or loss of RTA function. For example, KSHV RTA-induced m^6A mediates its pre-mRNA splicing, thus facilitating viral lytic replication (Ye et al., 2017). Histone acetylation modification at RTA promoter strongly reactivates MHV-68 from latency (Yang et al., 2009), and SUMOylation increases the transactivation activity of RTA (Chang et al., 2004). In the current study, deamidation

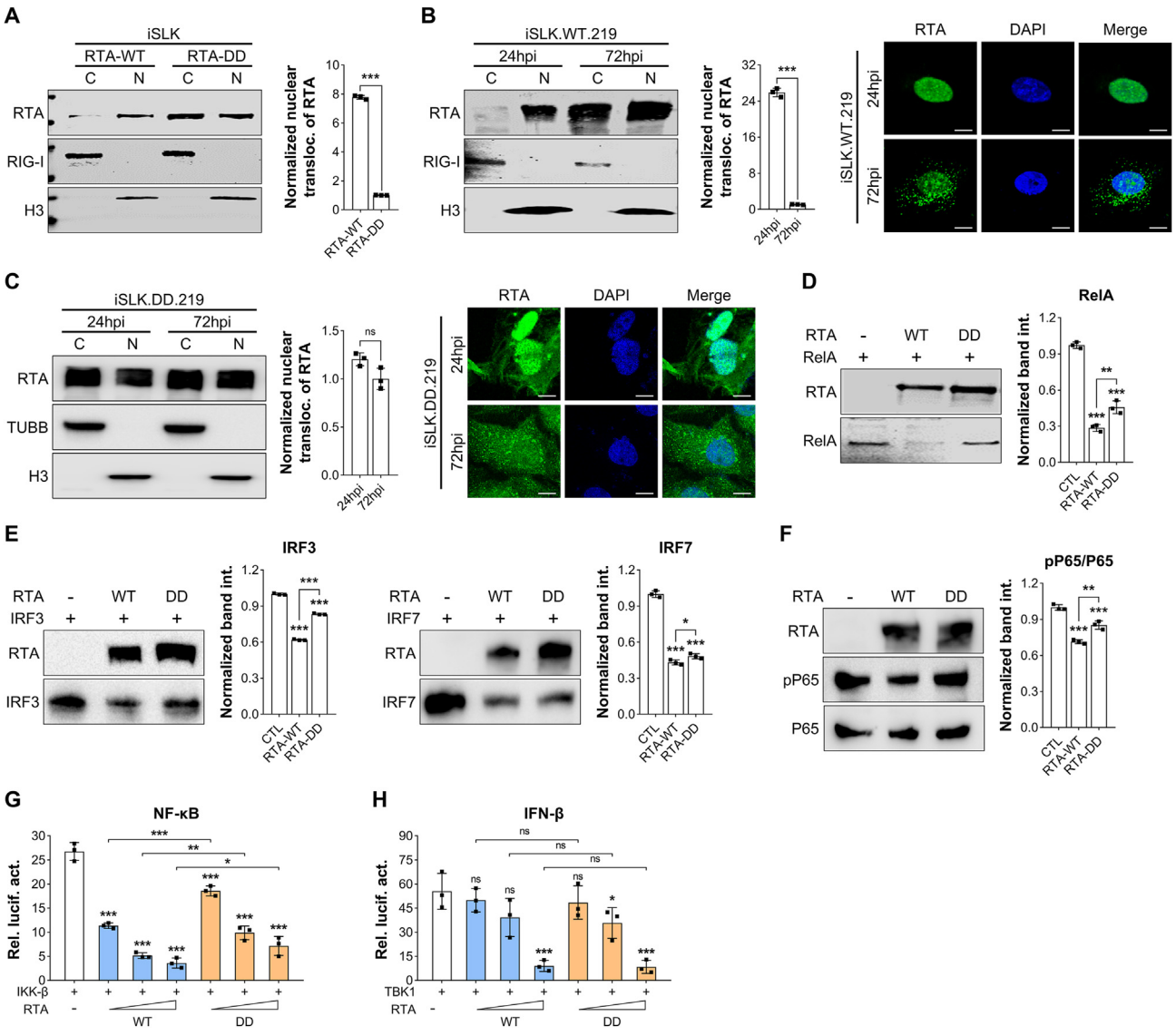

Fig. 5. Deamidation blocks RTA nuclear translocation and alleviates RTA-mediated suppression of NF-κB signaling. **A** iSLK cells stably expressing RTA-WT or RTA-DD were harvested, sequentially centrifuged to obtain cytosolic (C) and nuclear (N) fractions, and analyzed by immunoblotting with the indicated antibodies (left). The band intensity of RTA (N) /RTA (C) was normalized to quantify RTA nuclear localization (right). **B, C** iSLK.WT.219 cells were induced with doxycycline (1 μg/mL) for the indicated times. Cells were harvested, sequentially centrifuged to obtain cytosolic (C) and nuclear (N) fractions, and analyzed by immunoblotting with the indicated antibodies (left). The band intensity of RTA (N)/RTA (C) was normalized to quantify RTA nuclear localization (right). Cells were fixed and analyzed by fluorescence microscope. **D-F** 239T cells were transfected with equivalent doses of the indicated plasmids and harvested to detect the indicated protein expression by immunoblotting (left). The band intensity of the indicated protein was normalized to quantify protein expression (right). **G, H** 293T cells were transfected with indicated reporter cocktails and different dose of plasmids expressing RTA-WT or RTA-DD (0 ng, 4 ng, 8 ng, and 16 ng) with TBK1 (1 ng) or IKK-β (1 ng). Deamidation mediated RTA-dependent transcriptional activation of the indicated promoters was determined by luciferase reporter assay. Data presented as mean ± standard deviations. Statistical analyses were performed using Student's *t*-test or one-way analysis of variance (ANOVA). Statistical significance was set at $^{*}P < 0.05$, $^{**}P < 0.01$, $^{***}P < 0.001$, while "ns" indicated "not significant".

impairs RTA-mediated transcriptional activation of viral ORFs, blocks RTA nuclear translocation, and thus inactivates KSHV lytic replication. Inhibition of deamidation, in contrast, yields the opposite result. This result is consistent with our previous findings (Li et al., 2019), indicating that deamidation modification resulted in loss of function, whereas inhibition of deamidation leads to gain of function. Several studies have established the crosstalk of deamidation with other post-translational modifications. For instance, glycopeptide and glycoprotein deamidation are subject to the regulation of N-linked glycosylation (Zhu et al., 2020). Deamidation of asparagine (N14) arrests serine (S15) phosphorylation of cardiac myosin regulatory light chain (MLC2V) in humans (Goldspink et al., 2020). However, despite the fact that the impact of several post-translational modifications on RTA function has been preliminarily elucidated, the crosstalk of RTA deamidation with other post-translational modifications remains largely unclear and awaits future studies to establish. Notably, deamidation also alleviates RTA-induced repression of NF-κB signaling activation; this repression inhibits gamma-herpesvirus lytic replication (Brown et al., 2003). However, despite the fact that deamidation alleviates RTA-induced protein levels of IRFs, it is insufficient to alleviate the IFN-β promoter transcriptional activation, indicating that deamidation failed to rescue RTA-induced suppression of IFN signaling activation. Hence, RTA deamidation might regulate host antiviral immunity only to a certain extent during KSHV infection.

In the current study, it was identified that vGAT might inhibit the deamidation of other viral ORFs, such as ORF45, ORF59, and ORFK9.

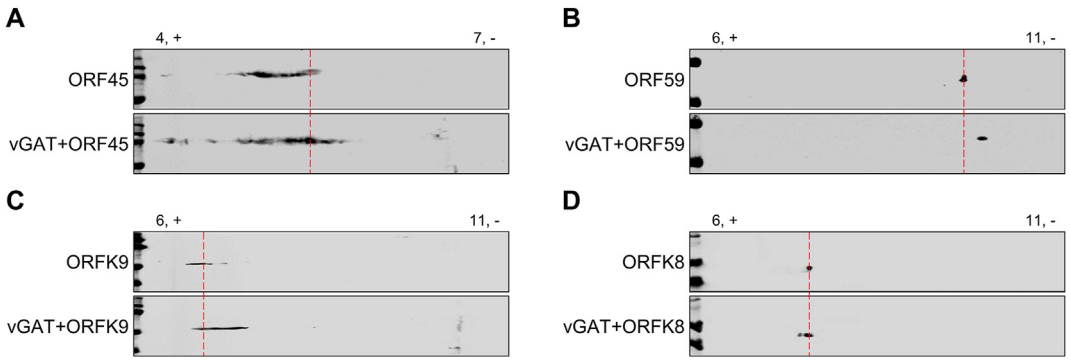

Fig. 6. vGAT inhibits the deamidation of KSHV lytic ORFs. **A**–**D** 293T cells were transfected with plasmids expressing the indicated genes without or with vGAT. WCLs were analyzed by two-dimensional gel electrophoresis and immunoblotting.

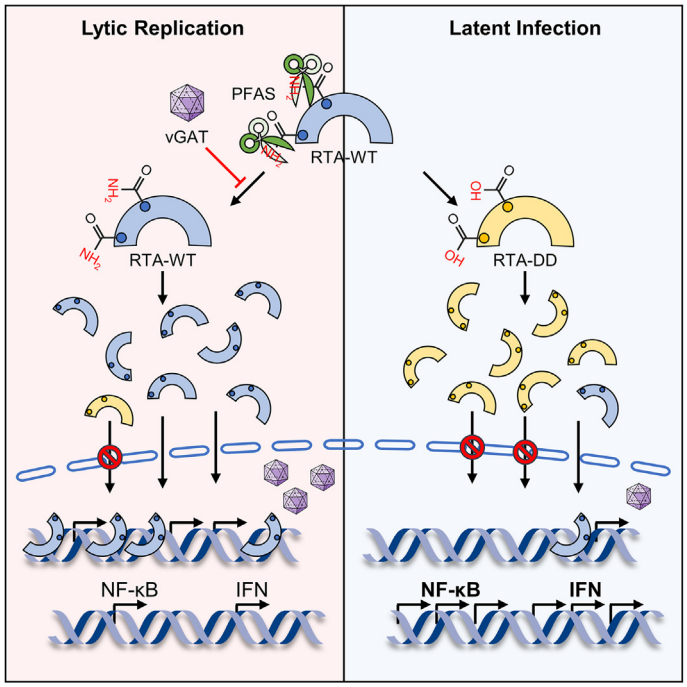

Fig. 7. Graphical abstract. A model depicting that vGAT was exploited by KSHV to competitively interact with RTA and cellular PFAS, thus suppressing PFAS-mediated RTA deamidation. Inhibition of deamidation enhanced RTA-mediated transcriptional activation and expression of viral ORFs, promoted RTA nuclear localization, and reinforced RTA-mediated suppression of NF-κB signaling, thus facilitating viral lytic replication.

ORF45 is a multifunctional immediate early and tegument protein of KSHV that modulates host immune responses and remodels signaling through phosphorylation, SUMOylation, and ubiquitination (Liang and Zhu, 2023; Liu et al., 2021, 2022; Alzhanova et al., 2021). ORF59 is the KSHV DNA polymerase processivity factor that is vital for viral reactivation and lytic replication. Several studies have revealed that ORF59 binds to oriLyt and mediates KSHV DNA synthesis in an RTA-dependent manner (Liu et al., 2008; Rossetto et al., 2011), and the interaction between ORF59 and RTA is regulated by phosphorylation (McDowell et al., 2013). ORFK9 encodes viral IRF1 (vIRF1), sharing homology with cellular IRF1, and is involved in the modulation of host immunity. The acetylation of vIRF1 could suppress host IFN signaling (Shi et al., 2023), and the inhibition of vIRF1-induced p53 acetylation and Hdm2 phosphorylation could impair the cellular p53-mediated antiviral response (Chavoshi et al., 2016). It was speculated that the inhibition of the deamidation of these viral ORFs by vGAT might also facilitate KSHV lytic replication. However, further investigations are warranted to validate this hypothesis.

CONCLUSIONS

In the current study, we report that vGAT is exploited to promote KSHV lytic infection by inhibiting RTA deamidation. Mechanistically, vGAT interactes with both RTA and cellular PFAS, and inhibits PFAS-mediated RTA deamidation, thus facilitating RTA nuclear localization and suppressing NF-κB signaling activation, as well as enhancing RTA-mediated transcriptional activation of viral ORFs (Fig. 7). Collectively, our work may provide valuable insights into potential strategies for tackling KSHV infection.

MATERIAL AND METHODS

Reagents

Detailed methods and reagent information are available in the Supplementary Material.

Cell maintenance and stable cell line generation

HEK293T and SLK cells (preserved in laboratory of Prof. Pinghui Feng) were maintained in DMEM supplemented with FBS (10%), penicillin (100 U/mL), and streptomycin (100 μg/mL). HOK cells (preserved in laboratory of Prof. Ren Sun) were maintained in Keratinocyte Growth Medium. The establishment of iSLK.RTA-WT and iSLK.RTA-DD stable cell lines were conducted as previously described (Li et al., 2019).

Site-directed mutagenesis

The codon encoding the asparagine residue (N) of RTA was mutated to aspartate (D) or glutamine (Q) using a commercial kit and confirmed by sequencing. Mutagenesis of iBAC16 was performed as previously described (Li et al., 2019). iBAC DNA was isolated using a commercial kit. All primers were listed in Supplementary Table S2.

DNA transfection and luciferase reporter assay

Polyethyleneimine (PEI) was used for the transfection of 293T cells. 293T cells were transfected with pPAN, pORF57, or pvIL-6 promoter reporter cocktails (100 ng) and different doses of plasmids expressing vGAT (1 ng, 10 ng, and 50 ng) without or with RTA (1 ng). 293T cells were transfected with pPAN, pORF57, or pvIL-6 promoter reporter cocktails (100 ng) and different doses of plasmids expressing RTA-WT, RTA-DD, or RTA-N37Q (2 ng, 4 ng, and 8 ng). 293T cells were transfected with IFN-β or NF-κB promoter reporter cocktails (100 ng) and different doses of plasmids expressing RTA-WT or RTA-DD (0 ng, 4 ng, 8 ng, and 16 ng) with TBK1 or IKK-β (1 ng). For iBAC DNA transfection into SLK and HOK cells, Lipofectamine 3000 was used. SLK.iBAC and HOK.iBAC-positive cells were selected with hygromycin B. At 30 h post-transfection, cells were harvested and luciferase activity was determined using a commercial kit.

Two-dimensional gel electrophoresis

Sample proteins were isolated and dissolved in 150 μL rehydration buffer. After centrifugation (20,000×*g*, 30 min), the supernatant was subjected to isoelectric focusing, and incubated with SDS equilibration buffer containing dithiothreitol (70 mmol/L) and 2-iodoacetamide (25 μg/mL) for 15 min, respectively. Washed with SDS-PAGE buffer, strips were resolved by SDS-PAGE and analyzed by immunoblotting.

Subcellular fractionation and immunofluorescence microscopy

Subcellular fractionation was performed as previously described (Li et al., 2019). Proteins obtained from cytoplasmic and nuclear fractions were analyzed by SDS-PAGE and immunoblotting with indicated antibodies, respectively. Immunofluorescence analysis was performed as previously described (Li et al., 2019). The treated slides were directly analyzed with a confocal microscope, and representative views were presented for all analysis.

Mass spectrometry analysis

RTA was purified from 293T cells transfected with a plasmid expressing RTA without or with vGAT by SDS-PAGE and Coomassie staining. Mass spectrometry (MS) analysis was performed by the Taplin Mass Spectrometry Facility.

Coimmunoprecipitation (CO-IP) and immunoblotting

CO-IP were performed as previously described (Li et al., 2019). Treated samples were subjected to SDS-PAGE and immunoblotting. All immunoblotting analysis were performed using the indicated primary antibodies and secondary antibodies and visualized.

Quantitative real-time PCR (qPCR)

Reactivated iSLK.219 and HOK.iBAC cells were extracted using TRIzol reagent and transcripted into cDNA using a commercial kit. qPCR was performed using a commercial kit. The relative mRNA expressions of targeted genes were calculated using the $2^{-\Delta\Delta Ct}$ method and normalized to the expression levels of β-Actin. All primers were listed in Supplementary Table S2.

Statistical analysis

All data were presented as mean ± standard deviations (SD). Statistical analysis was performed using Student's *t*-test or one-way analysis of variance (ANOVA). Statistical significance was set at $^{*}P < 0.05$, $^{**}P < 0.01$, $^{***}P < 0.001$, while "ns" indicated "not significant".

DATA AVAILABILITY

All the data generated during the current study are included in the manuscript and supplementary data.

ETHICS STATEMENT

This article does not contain any studies with human or animal subjects performed by any of the authors.

AUTHOR CONTRIBUTIONS

Yang Xu: data curation, formal analysis, investigation, software, visualization, writing-original draft. Qiushi Zhang: data curation, formal analysis, investigation, software, visualization, writing-original draft. Guoli Hou: investigation, data curation, validation. Liang Hu: investigation, data curation, validation. Tiaoyi Xiao: resources. Deliang Li: project administration, funding acquisition, supervision. Junhua Li: conceptualization, methodology, project administration, funding acquisition, supervision, writing-review & editing.

CONFLICT OF INTEREST

The authors declare that they have no conflict of interest.

ACKNOWLEDGMENTS

We thank Dr. Pinghui Feng (University of Southern California) and Dr. Jun Zhao (Cleveland Clinic) for providing reagents and resources. This work was funded by the National Natural Science Foundation of China (32173021), the Natural Science Foundation of Hunan Province (2024JJ5184), the Hunan Provincial Science & Technology Major Project (2022sfq30, 20231F18), the Key Projects of Hunan Provincial Education Department (23A0196), and the Earmarked Fund for Hunan Agriculture Research System (HARS-07).

APPENDIX A. SUPPLEMENTARY DATA

Supplementary data to this article can be found online at https://doi.org/10.1016/j.virs.2025.04.005.

REFERENCES

Alzhanova, D., Meyo, J.O., Juarez, A., Dittmer, D.P., 2021. The ORF45 protein of Kaposi sarcoma-associated herpesvirus is an inhibitor of p53 signaling during viral reactivation. J. Virol. 95, e0145921.

Arias, C., Weisburd, B., Stern-Ginossar, N., Mercier, A., Madrid, A.S., Bellare, P., Holdorf, M., Weissman, J.S., Ganem, D., 2014. KSHV 2.0: a comprehensive annotation of the Kaposi's sarcoma-associated herpesvirus genome using next-generation sequencing reveals novel genomic and functional features. PLoS Pathog. 10, e1003847.

Broussard, G., Damania, B., 2020. Regulation of KSHV latency and lytic reactivation. Viruses 12, 1034.
Brown, H.J., Song, M.J., Deng, H., Wu, T.T., Cheng, G., Sun, R., 2003. NF-kappaB inhibits gammaherpesvirus lytic replication. J. Virol. 77, 8532–8540.
Chang, L.K., Lee, Y.H., Cheng, T.S., Hong, Y.R., Lu, P.J., Wang, J.J., Wang, W.H., Kuo, C.W., Li, S.S., Liu, S.T., 2004. Post-translational modification of Rta of Epstein-Barr virus by SUMO-1. J. Biol. Chem. 279, 38803–38812.
Chang, Y., Cesarman, E., Pessin, M.S., Lee, F., Culpepper, J., Knowles, D.M., Moore, P.S., 1994. Identification of herpesvirus-like DNA sequences in AIDS-associated Kaposi's sarcoma. Science 266, 1865–1869.
Chavoshi, S., Egorova, O., Lacdao, I.K., Farhadi, S., Sheng, Y., Saridakis, V., 2016. Identification of Kaposi sarcoma herpesvirus (KSHV) vIRF1 protein as a novel interaction partner of human deubiquitinase USP7. J. Biol. Chem. 291, 6281–6291.
Combs, L.R., Spires, L.M., Alonso, J.D., Papp, B., Toth, Z., 2022. KSHV RTA induces degradation of the host transcription repressor ID2 to promote the viral lytic cycle. J. Virol. 96, e0010122.
Goldspink, P., Martin, J.L., Warren, C.M., Thompson, W., Levi-D'Ancona, E., de Tombe, P.P., 2020. Deamidation of asparagine14 prevents serine15 phosphorylation of human cardiac MLC2V. Biophys. J. 118, 593a.
Han, C., Zhang, D., Gui, C., Huang, L., Chang, S., Dong, L., Bai, L., Wu, S., Lan, K., 2022. KSHV RTA antagonizes SMC5/6 complex-induced viral chromatin compaction by hijacking the ubiquitin-proteasome system. PLoS Pathog. 18, e1010744.
He, S., Zhao, J., Song, S., He, X., Minassian, A., Zhou, Y., Zhang, J., Brulois, K., Wang, Y., Cabo, J., Zandi, E., Liang, C., Jung, J.U., Zhang, X., Feng, P., 2015. Viral pseudo-enzymes activate RIG-I via deamidation to evade cytokine production. Mol. Cell 58, 134–146.
Li, J., Zhao, J., Xu, S., Zhang, S., Zhang, J., Xiao, J., Gao, R., Tian, M., Zeng, Y., Lee, K., Tarakanova, V., Lan, K., Feng, H., Feng, P., 2019. Antiviral activity of a purine synthesis enzyme reveals a key role of deamidation in regulating protein nuclear import. Sci. Adv. 5, eaaw7373.
Liang, Q., Zhu, F., 2023. ORF45, a multifunctional immediate early and tegument protein of KSHV. J. Med. Virol. 95, e28659.
Liu, Y., Cao, Y., Liang, D., Gao, Y., Xia, T., Robertson, E.S., Lan, K., 2008. Kaposi's sarcoma-associated herpesvirus RTA activates the processivity factor ORF59 through interaction with RBP-Jkappa and a cis-acting RTA responsive element. Virology 380, 264–275.
Liu, Z., Liu, C., Wang, X., Li, W., Zhou, J., Dong, P., Xiao, M.Z.X., Wang, C., Zhang, Y., Fu, J., Zhu, F., Liang, Q., 2021. RSK1 SUMOylation is required for KSHV lytic replication. PLoS Pathog. 17, e1010123.
Liu, Z., Wang, X., Liu, C., Deng, H., Li, W., Wang, X., Xu, X., Xiao, M.Z.X., Wang, C., Zhang, Y., Fu, J., Zhu, F., Liang, Q., 2022. The SUMO E3 ligase activity of ORF45 determines KSHV lytic replication. PLoS Pathog. 18, e1010504.
Lu, A., Disoma, C., Zhou, Y., Chen, Z., Zhang, L., Shen, Y., Zhou, M., Du, A., Zheng, R., Li, S., Alsaadawe, M., Li, S., Li, J., Wang, W., Jiang, T., Peng, J., Xia, Z., 2019. Protein interactome of the deamidase phosphoribosylformylglycinamidine synthetase (PFAS) by LC-MS/MS. Biochem. Biophys. Res. Commun. 513, 746–752.
McDowell, M.E., Purushothaman, P., Rossetto, C.C., Pari, G.S., Verma, S.C., 2013. Phosphorylation of Kaposi's sarcoma-associated herpesvirus processivity factor ORF59 by a viral kinase modulates its ability to associate with RTA and oriLyt. J. Virol. 87, 8038–8052.
Olson, A.T., Wang, Z., Rico, A.B., Wiebe, M.S., 2019. A poxvirus pseudokinase represses viral DNA replication via a pathway antagonized by its paralog kinase. PLoS Pathog. 15, e1007608.
Qin, C., Rao, Y., Yuan, H., Wang, T.Y., Zhao, J., Espinosa, B., Liu, Y., Zhang, S., Savas, A.C., Liu, Q., Zarinfar, M., Rice, S., Henley, J., Comai, L., Graham, N.A., Chen, C., Zhang, C., Feng, P., 2022. SARS-CoV-2 couples evasion of inflammatory response to activated nucleotide synthesis. Proc. Natl. Acad. Sci. U. S. A 119, e2122897119.
Rao, Y., Wang, T.Y., Qin, C., Espinosa, B., Liu, Q., Ekanayake, A., Zhao, J., Savas, A.C., Zhang, S., Zarinfar, M., Liu, Y., Zhu, W., Graham, N., Jiang, T., Zhang, C., Feng, P., 2021. Targeting CTP synthetase 1 to restore interferon induction and impede nucleotide synthesis in SARS-CoV-2 infection. mBio. https://doi.org/10.1128/mbio.00649-25.
Rico, A.B., Linville, A.C., Olson, A.T., Wang, Z., Wiebe, M.S., 2021. The vaccinia virus B12 pseudokinase represses viral replication via interaction with the cellular kinase VRK1 and activation of the antiviral effector BAF. J. Virol. 95, e02114-20.
Rico, A.B., Wang, Z., Olson, A.T., Linville, A.C., Bullard, B.L., Weaver, E.A., Jones, C., Wiebe, M.S., 2019. The vaccinia virus (VACV) B1 and cellular VRK2 kinases promote VACV replication factory formation through phosphorylation-dependent inhibition of VACV B12. J. Virol. 93, e00855-19.
Rossetto, C.C., Susilarini, N.K., Pari, G.S., 2011. Interaction of Kaposi's sarcoma-associated herpesvirus ORF59 with oriLyt is dependent on binding with K-Rta. J. Virol. 85, 3833–3841.
Shi, J., Jia, X., He, Y., Ma, X., Qi, X., Li, W., Gao, S.J., Yan, Q., Lu, C., 2023. Immune evasion strategy involving propionylation by the KSHV interferon regulatory factor 1 (vIRF1). PLoS Pathog. 19, e1011324.
Spires, L.M., Wind, E., Papp, B., Toth, Z., 2023. KSHV RTA utilizes the host E3 ubiquitin ligase complex RNF20/40 to drive lytic reactivation. J. Virol. 97, e0138923.
Sun, R., Lin, S.F., Gradoville, L., Yuan, Y., Zhu, F., Miller, G., 1998. A viral gene that activates lytic cycle expression of Kaposi's sarcoma-associated herpesvirus. Proc. Natl. Acad. Sci. U. S. A 95, 10866–10871.
Teoh, M.L., Turner, P.V., Evans, D.H., 2005. Tumorigenic poxviruses up-regulate intracellular superoxide to inhibit apoptosis and promote cell proliferation. J. Virol. 79, 5799–5811.
Tian, H., Yu, K., He, L., Xu, H., Han, C., Zhang, X., Wang, X., Zhang, X., Zhang, L., Gao, G., Deng, H., 2023. RNF213 modulates γ-herpesvirus infection and reactivation via targeting the viral replication and transcription activator. Proc. Natl. Acad. Sci. U. S. A 120, e2218825120.
Wan, Q., Tavakoli, L., Wang, T.Y., Tucker, A.J., Zhou, R., Liu, Q., Feng, S., Choi, D., He, Z., Gack, M.U., Zhao, J., 2024. Hijacking of nucleotide biosynthesis and deamidation-mediated glycolysis by an oncogenic herpesvirus. Nat. Commun. 15, 1442.
Wang, S., Tian, X., Zhou, Y., Xie, J., Gao, M., Zhong, Y., Zhang, C., Yu, K., Bai, L., Qin, Q., Zhong, B., Lin, D., Feng, P., Lan, K., Zhang, J., 2024. Non-canonical regulation of the reactivation of an oncogenic herpesvirus by the OTUD4-USP7 deubiquitinases. PLoS Pathog. 20, e1011943.
Wang, T.Y., Zhao, J., Savas, A.C., Zhang, S., Feng, P., 2020. Viral pseudoenzymes in infection and immunity. FEBS J. 287, 4300–4309.
Xie, T., Qin, C., Savas, A.C., Yeh, W.W., Feng, P., 2024. The emerging roles of glutamine amidotransferases in metabolism and immune defense. Nucleosides Nucleotides Nucleic Acids 43, 783–797.
Xu, Y., Hou, G., Liu, Q., Zhang, Q., Li, C., Hu, L., Chen, X., Chen, R., Ding, C., Li, D., Li, J., 2023. Helicase-independent function of RIG-I against murine gammaherpesvirus 68 via blocking the nuclear translocation of viral proteins. Int. J. Biol. Macromol. 250, 126527.
Yang, X., Zhou, J., Liu, C., Qu, Y., Wang, W., Xiao, M.Z.X., Zhu, F., Liu, Z., Liang, Q., 2022. KSHV-encoded ORF45 activates human NLRP1 inflammasome. Nat. Immunol. 23, 916–926.
Yang, Z., Tang, H., Huang, H., Deng, H., 2009. RTA promoter demethylation and histone acetylation regulation of murine gammaherpesvirus 68 reactivation. PLoS One 4, e4556.
Ye, F., Chen, E.R., Nilsen, T.W., 2017. Kaposi's Sarcoma-associated herpesvirus utilizes and manipulates RNA N^6-adenosine methylation to promote lytic replication. J. Virol. 91, e00466-17.
Ye, F., Lei, X., Gao, S.J., 2011. Mechanisms of Kaposi's sarcoma-associated herpesvirus latency and reactivation. Adv. Virol. 2011, 193860.
Yu, Y., Wang, S.E., Hayward, G.S., 2005. The KSHV immediate-early transcription factor RTA encodes ubiquitin E3 ligase activity that targets IRF7 for proteosome-mediated degradation. Immunity 22, 59–70.
Zhang, J., Zhao, J., Xu, S., Li, J., He, S., Zeng, Y., Xie, L., Xie, N., Liu, T., Lee, K., Seo, G.J., Chen, L., Stabell, A.C., Xia, Z., Sawyer, S.L., Jung, J., Huang, C., Feng, P., 2018. Species-specific deamidation of cGAS by herpes simplex virus UL37 protein facilitates viral replication. Cell Host Microbe 24, 234–248.e5.
Zhang, Y., Dong, Z., Gu, F., Xu, Y., Li, Y., Sun, W., Rao, W., Du, S., Zhu, C., Wang, Y., Wei, F., Cai, Q., 2024. Degradation of TRIM32 is induced by RTA for Kaposi's sarcoma-associated herpesvirus lytic replication. J. Virol. 98, e0000524.
Zhao, J., Li, J., Xu, S., Feng, P., 2016a. Emerging roles of protein deamidation in innate immune signaling. J. Virol. 90, 4262–4268.
Zhao, J., Tian, M., Zhang, S., Delfarah, A., Gao, R., Rao, Y., Savas, A.C., Lu, A., Bubb, L., Lei, X., Moshirian, R., Zhu, W., Peng, C., Jiang, T., Chen, L., Graham, N.A., Feng, P., 2020. Deamidation shunts RelA from mediating inflammation to aerobic glycolysis. Cell Metab. 31, 937–955.e7.
Zhao, J., Zeng, Y., Xu, S., Chen, J., Shen, G., Yu, C., Knipe, D., Yuan, W., Peng, J., Xu, W., Zhang, C., Xia, Z., Feng, P., 2016b. A viral deamidase targets the helicase domain of RIG-I to block RNA-induced activation. Cell Host Microbe 20, 770–784.
Zhao, Q., Liang, D., Sun, R., Jia, B., Xia, T., Xiao, H., Lan, K., 2015. Kaposi's sarcoma-associated herpesvirus-encoded replication and transcription activator impairs innate immunity via ubiquitin-mediated degradation of myeloid differentiation factor 88. J. Virol. 89, 415–427.
Zhu, H.J., Liu, D., Tran, V.P., Wu, Z., Jiang, K., Zhu, H., Zhang, J., Gibbons, C., Xue, B., Shi, H., Wang, P.G., 2020. N-linked glycosylation prevents deamidation of glycopeptide and glycoprotein. ACS Chem. Biol. 15, 3197–3205.